Broadband Electromagnetic Induction Sensor for Detecting Buried Landmines

Waymond R. Scott, Jr.

School of Electrical and Computer Engineering
Georgia Institute of Technology
Atlanta, Georgia 30332-0250
waymond.scott@ece.gatech.edu

Abstract— **A broadband electromagnetic induction (EMI) sensor is developed to help discriminate between buried land mines and metal clutter. The detector uses simple dipole transmit and receive coils along with a secondary bucking transformer to mostly cancel the coupling between the coils. The technique allows the cancellation that can be obtained using a quadrupole receive coil while maintaining the depth sensitivity and simple detection zone of a dipole coil. Experimental results are presented for several targets.**

Keywords; Electromagnetic Induction, EMI, Mine, Lansmine, Metal Detector.

I. INTRODUCTION

For many years, extensive effort has been expended developing techniques for efficiently locating buried landmines. For a mine detection technique to be successful there must be sufficient contrast between the properties of the mine and the earth. There also must be sufficient contrast between the properties of the mine and common types of clutter such as rocks, roots, cans, etc. so that the mine can be distinguished from the clutter. The latter condition is the most problematic for most mine detection techniques. For example, simple electromagnetic induction (EMI) sensors are capable of detecting most mines; however, they will also detect every buried metal object such as bottle tops, nails, shrapnel, bullets, etc. This results in an unacceptable false alarm rate. This is even more problematic for low-metal anti-personnel mines as they are extremely difficult to distinguish from clutter using a simple EMI sensor. In recent years, advanced EMI sensors that use a broad range of frequencies or a broad range of measurement times along with advanced signal processing have been shown to be capable of discrimination between buried land mines and many types of buried metal clutter [1-4]. For these advanced EMI sensors to be effective, they must be able to accurately, repeatably, and quickly measure the response of a buried target. This is difficult because the sensor must operate with bandwidths greater than 100 to 1 while accurately measuring signals that are more than 100 dB smaller than the direct coupling between the coils on the EMI sensor. In order to accomplish this, the EMI sensor must be very
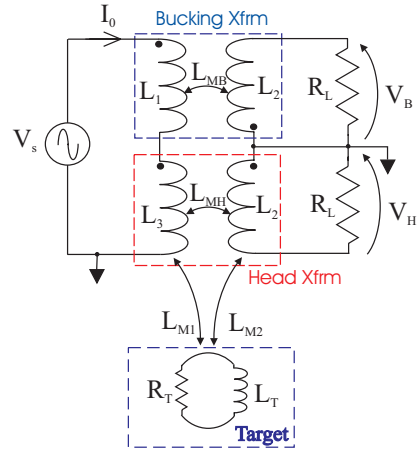
Figure 1. Basic configuration of the technique.

cleverly designed to account for the coupling and for the secondary effects such as resonances in the coils.

In most EMI sensors, the coupling between the coils is handled by one of two methods. In time-domain sensors, the coupling between the coils can be mostly removed by time gating if the coils are properly designed. In frequency-domain sensors, the coupling is mostly removed by using a quadrupole receive coil which minimizes the mutual inductance between the coils. The quadrupole receive coils have the disadvantage of being less sensitive to deeply buried targets and having a complicated detection zone when compared to a dipole receive coil.

A technique is presented for canceling the coupling between the induction coils while maintaining the depth sensitivity and simple detection zone of a dipole coil. Here, simple dipole transmit and receive coils are used along with a secondary bucking transformer to cancel the coupling between the coils. A prototype system using this technique is presented that operates over the frequency range 300 Hz to 90 kHz. Sample measurements made with the system are shown.

EMI Head

Constructed using
PCB Technology

Summing Network/ Pre-
Amplifiers/ Bucking
Transformer

Figure 2. Prototype EMI System

Conductive
Bus

Conductive rings

Gap

Figure 3. Diagram of the shield for the EMI head.

II. System

Figure 1 shows a basic diagram of the system where simple dipole transmit and receive coils are used along with a secondary transformer to cancel the direct coupling between the coils. Here, the exciting current I_o passes through the primary coils of both the bucking and head transformers and induces a voltage in the secondary transformers. The voltage induced in the secondary windings of the head transformer depends on its mutual inductance as well as the coupling through the target:

$$V_H = j\omega L_{MH} I_0 - \frac{\omega^2 L_{M1} L_{M2}}{R_T + j\omega L_T} I_0 .$$

The first term in the equation above is due to the direct coupling between the coils of the head transformer, and it is generally much larger than the second term which is due to the target. The voltage induced in the secondary windings of the bucking transformer depends only on its mutual inductance:

$$V_B = -j\omega L_{MB} I_0 .$$

The response of the target is obtained from the relation

$$R = \frac{V_H + V_B}{V_B} = \frac{j\omega L_{M1} L_{M2}}{L_{MB}(R_T + j\omega L_T)}$$

if we make $L_{MH}=L_{MB}$. This is the ideal response (scaled by L_{MB}, L_{M1}, and L_{M2}) that we want to obtain with the direct coupling term eliminated. It is difficult to exactly match the mutual inductances, so a simple voltage divider is used to compensate for the difference. The transformers are not ideal and will have significant parasitic effects such as the distributed capacitance between the windings. The parasitic elements can significantly reduce the effectiveness of the cancellation at the higher frequencies. Additional elements were added to the circuit to mostly match the parasitics effects for the two transformers. With these additional elements the resulting cancellation was greater than 60 dB across the entire frequency range. To further enhance the cancellation, the response of the sensor in air is subtracted from the subsequent measurements. After the subtraction the effective cancellation is approximately 120 dB over the entire bandwidth of the sensor.
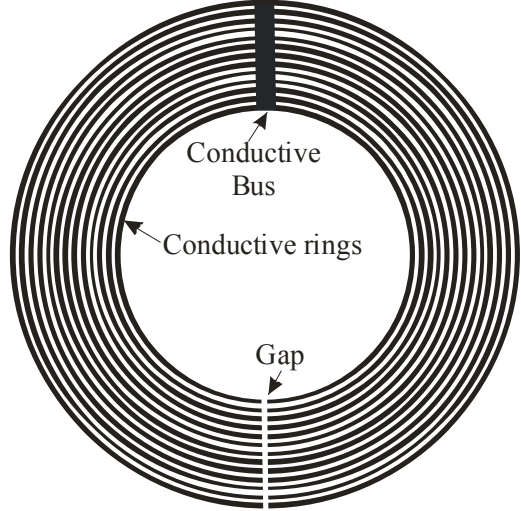
The prototype system consists of a head constructed using PCB technology that has a transmit coil with a diameter of approximately 25 cm and a receive coil with a diameter of approximately 21 cm, as shown in Figure 2. This is an improved version of the system presented previously [6]. The improvements include improved shielding of the EMI head and a much smaller bucking transformer made using a ferrite core.

The coupling between the transmit and receive coils is not purely inductive as in the model, figure 1. Part of the coupling is due to the capacitance between the transmit and receive coils. The capacitive coupling can be comparable to or larger than the inductive coupling with the target. The capacitive coupling can vary significantly as an unshielded EMI head is moved in close proximity to the soil and can mask/corrupt the inductive responses of the desired targets. The effect is most problematic at the higher frequencies. Ideally, the shield will completely eliminate the variations in the capacitive coupling due to the presence of the soil or other objects that are in close proximity to the head while not affecting the inductive coupling to the target. The shield developed for this work is shown in figure 3. The shield is made using PCB technology and consists of closely spaced conducting rings with a gap so the rings will not form closed loops. The narrow width of the rings and the gap in the rings greatly reduce the eddy currents induced on the shield. The eddy currents are undesirable because they corrupt the desired inductive response. This shield has performed much better than the conductive Mylar shield used in the previous work.

The data for the prototype system was taken at 21 frequencies that were approximately logarithmically spaced from 330 HZ to 90.03 KHz. The frequencies deviated from logarithmic spacing to minimize interference from power line harmonics. A multi-sine excitation signal was generated using the 21 frequencies and used to excite the EMI sensor. The response due to this multi-sine excitation was recorded in 0.1 s increments. These time records were transformed into the frequency domain and used to construct the response of the sensor.
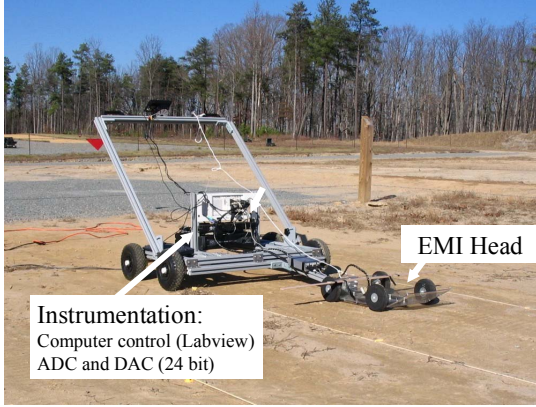
Figure 4. Cart based EMI data collection system.

III. EXPERIMETAL RESULTS

The prototype system was used to collect data at a test faculty. The test facility consisted of a number of lanes divided into 1.5 by 1.5 m squares. A target was buried at the center of most of the squares. The data was collected in a lane based manner in which the sensor was pushed down the lane and the response was recorded in 0.1 s time increments along with the spatial location in the grid. The response at the beginning of the grid is subtracted from the subsequent responses to partially remove the ground response.

The response for three of the target types is shown in figure 5 in two types of graphs. For the graphs in the left column, the response at the center of the grid square is graphed on Argand diagrams where the imaginary part of the response is graphed as a function of the real part with frequency as a parameter. The curves are shifted along the real axis so that they are centered; this further removes part of the ground response which is mostly a shift in the real part of the response. The response of a simple target with a single relaxation will form a perfect semicircle on this type of graph. The fidelity of the data is generally apparent on this type of graph so it is a good way to show the measured data. The shape of the curve is dependent on the shape of the buried object and can be used discriminate different targets from each other. These graphs are very similar to the Cole-Cole graphs commonly used to show the complex permittivity of materials with dipolar type relaxations.

The responses from eight different grid locations that contain TS-50 landmines with burial depths from 0 cm to 5 cm are plotted in figure 5a. The eight curves are almost perfect scaled replicas of each other which demonstrates the consistency and the fidelity of the EMI sensor. The curves form a portion of a semicircle indicating that this landmine has a single simple relaxation. Only part of the semicircle is evident because of the limited frequency range of the measurement. The variation in the size of the curves is due to the differences in burial depth. The responses from six different grid locations that contain MAI-75 landmines with burial depths from 0 cm to 5 cm are plotted in figure 5b. The shapes of the six curves are very similar to each other, again showing the consistency and the fidelity of the EMI sensor.

The shapes of these curves are more complex than a semicircle indicating that this landmine has multiple relaxations. The responses from three different grid squares which contain a buried 30 cm by 30 cm patio stone are shown in figure 5c. One would not expect to see a response from the patio stone, but it is clearly evident. The response may be due to the stone having a different conductivity [8] and/or permeability that the surrounding soil. Using the frequency dependent response of the targets, it is possible to discriminate between landmines and many types of clutter [9].
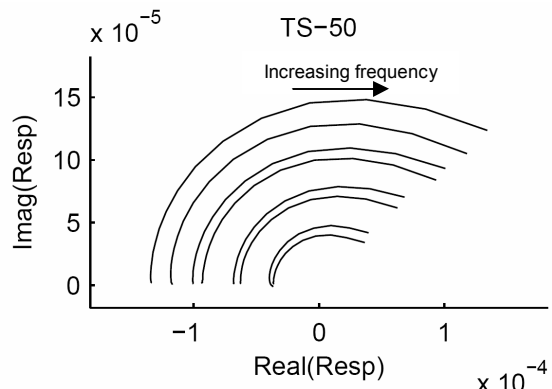
The graphs on the right column of figure 5 are the response as a function of distance along the centerline of the grid. The magnitude of the response is plotted for all 21 frequencies on these graphs. The response for these three graphs is peaked near the center of the grid and reaches a noise floor away from the center of the grid. The noise floor is seen to be approximately 120 dB below V_B. The peak response for the TS-50 mine is about 80 dB below V_B, for the MAI-75 mine is about 90 dB below V_B, and for the patio stone is about 110 dB below V_B.

IV. ACKNOWLEDGEMENT
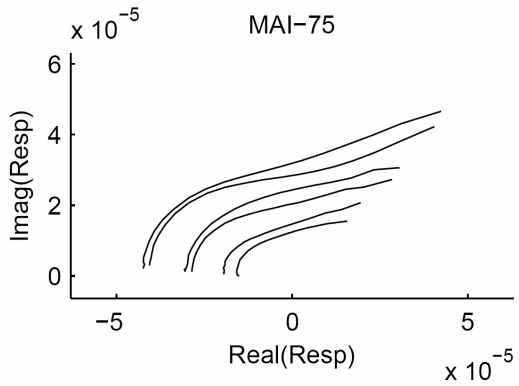
REFERENCES
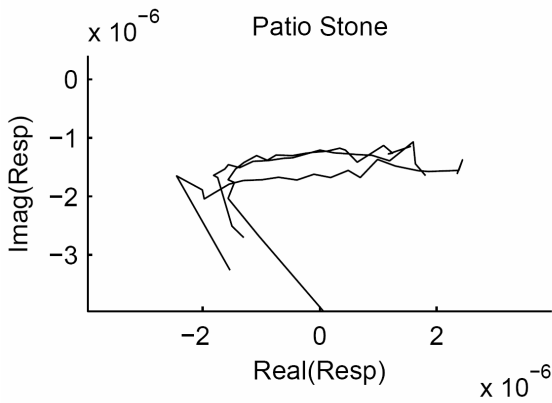
[1] P. Gao, L. Collins, P.M. Garber, N. Geng, and L. Carin, "Classification of Landmine-Like Metal Targets Using Wideband Electromagnetic Induction," *IEEE Transactions on Geoscience and Remote Sensing*, Vol. 38, No. 3, May 2000.

[2] L. Collins, P. Gao, and L. Carin, "An Improved Bayesian Decision Theoretic Approach for Land Mine Detection," *IEEE Transactions on Geoscience and Remote Sensing*, Vol. 37, No. 2, March 1999.

[3] G. D. Sower and S. P. Cave, "Detection and identification of mines from natural magnetic and electromagnetic resonances," in *Proc. SPIE*, Orlando, FL, 1995.

[4] C. E. Baum, "Low Frequency Near-Field Magnetic Scattering from Highly, but Not Perfectly Conducting Bodies," Phillips Laboratory, *Interaction Note* 499, Nov. 1993.

[5] G.T. Mallick, Jr. W.J. Carr, Jr., and R.C. Miller, "Multiple Frequency Magnetic Field Technique for Differentiating between Classes of Metal Objects," U.S. Patent 3,686,564, Aug. 22, 1972.

[6] Scott, W.R., Jr. and Malluck, M., "New cancellation technique for electromagnetic induction sensors," *Proceedings of the SPIE: 2005 Annual International Symposium on Aerospace/Defense Sensing, Simulation, and Controls*, Vol. 5794, Orlando, FL, April 2005

[7] L.S. Riggs, L.T. Lowe, J.E. Mooney, T. Barnett, R. Ess, and F. Paca, "Simulants (decoys) for Low-Metallic Content Mines: Theory and Experimental Results," in *Proc. SPIE*, Vol. 3710, Orlando, FL, 1999.

[8] T. Yu and L. Carin, "Analysis of the electromagnetic inductive response of a void in a conducting-soil background," *IEEE Transactions on Geoscience and Remote Sensing*, Vol. 38, No. 3, May 2000.

[9] E.B. Fails, P.A. Torrione, W. R. Scott, Jr, and L.M. Collins, "Performance of a four parameter model for modeling landmine signatures in frequency domain wideband electromagnetic induction detection systems," *Proceedings of the SPIE: 2007 Annual International Symposium on Aerospace/Defense Sensing, Simulation, and Controls*, Vol. 6553, Orlando, FL, May 2007.
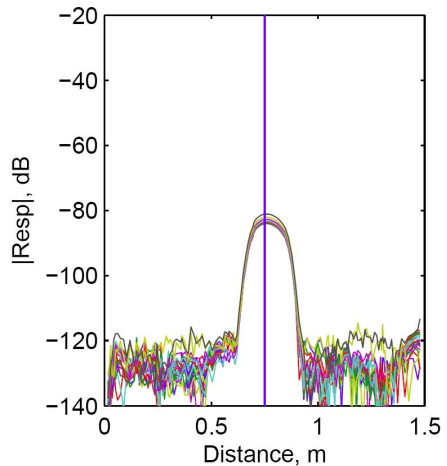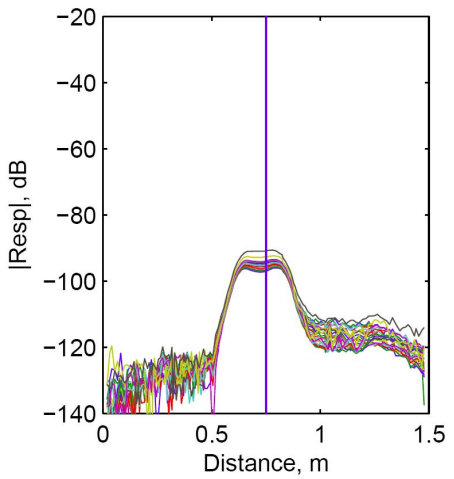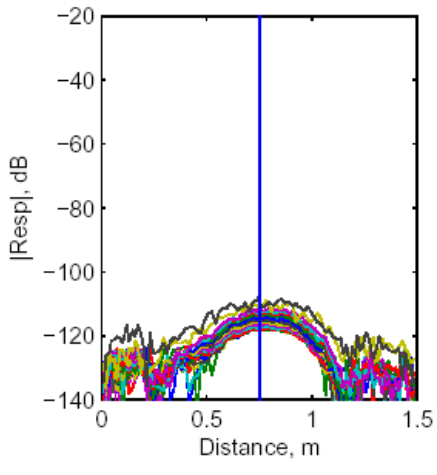
Figure 5. Response plotted on an Argand diagram over the center of a) TS-50 anti-personnel landmines buried 0 to 5 cm deep, b) MAI-75 anti-personnel landmines buried 0 to 5 cm deep, and c) patio stones buried 2.5 to 11 cm deep. Magnitude of the response at the 21 measurement frequencies plotted as a function of downtract distance for d) a TS-50 landmine buried 5 cm deep, e) a MAI-75 landmine buried 5 cm deep, and patio stone buried 7.5 cm deep.